Molecular basis of coiled-coil formation

Michel O. Steinmetz*†, Ilian Jelesarov‡, William M. Matousek§, Srinivas Honnappa*, Wolfgang Jahnke¶, John H. Missimer*, Sabine Frank‖, Andrei T. Alexandrescu§, and Richard A. Kammerer†**

*Biomolecular Research, Structural Biology, Paul Scherrer Institut, CH-5232 Villigen PSI, Switzerland; ‡Biochemisches Institut der Universität Zürich, Winterthurerstrasse 190, CH-8057 Zürich, Switzerland; §Department of Molecular and Cell Biology, University of Connecticut, Storrs, CT 06269-3125; ¶Central Technologies, Novartis Pharma AG, CH-4002 Basel, Switzerland; ‖F. Hoffmann-La Roche Ltd, CH-4070 Basel, Switzerland; and **Wellcome Trust Centre for Cell-Matrix Research, Faculty of Life Sciences, University of Manchester, Manchester M13 9PT, United Kingdom

Edited by Alan R. Fersht, University of Cambridge, Cambridge, United Kingdom, and approved March 7, 2007 (received for review January 12, 2007)

Coiled coils have attracted considerable interest as design templates in a wide range of applications. Successful coiled-coil design strategies therefore require a detailed understanding of coiled-coil folding. One common feature shared by coiled coils is the presence of a short autonomous helical folding unit, termed "trigger sequence," that is indispensable for folding. Detailed knowledge of trigger sequences at the molecular level is thus key to a general understanding of coiled-coil formation. Using a multidisciplinary approach, we identify and characterize here the molecular determinants that specify the helical conformation of the monomeric early folding intermediate of the GCN4 coiled coil. We demonstrate that a network of hydrogen-bonding and electrostatic interactions stabilize the trigger-sequence helix. This network is rearranged in the final dimeric coiled-coil structure, and its destabilization significantly slows down GCN4 leucine zipper folding. Our findings provide a general explanation for the molecular mechanism of coiled-coil formation.

autonomous folding unit | protein folding | trigger sequence | leucine zipper | α-helix

Although coiled coils have been used traditionally as model systems for protein folding studies, the molecular basis of how they fold is still largely unknown. A need for a detailed understanding of coiled-coil folding is relevant, particularly in light of the important functions these structures play in almost all biological processes, as well as the considerable attention coiled coils have recently garnered in a wide range of applications, including basic research, nanomaterials, protein engineering, biotechnology, and medicine (1–13). Furthermore, understanding the folding mechanisms of coiled coils is of fundamental interest to experimentalists and theoreticians challenged by the question of how the sequence of a protein defines its specific 3D structure. Along these lines, we have been interested particularly in coiled-coil "trigger sequences," which encode stable monomeric α-helices that are indispensable for coiled-coil formation (14–18). Although there are a few examples of synthetic peptides that fold either into heterodimers (19) or at conditions of extremes of pH (20) without an apparent trigger sequence, the "trigger site" concept is generally accepted because these short autonomous helical folding units are structurally and functionally conserved in a large number of native coiled-coil proteins (reviewed in refs. 21–24). Detailed knowledge of the properties of trigger sequences at the molecular level is therefore key to an understanding of coiled-coil formation and function in general.

The parallel two-stranded leucine zipper of the yeast transcriptional activator GCN4 is the best-characterized coiled coil and thus represents an excellent paradigm for a comprehensive analysis of the roles of trigger sequences in coiled-coil folding. Our current understanding of the folding kinetics of the GCN4 leucine zipper is based on extensive stopped-flow studies and temperature-jump experiments (25–28). Most of these studies reported simple bimolecular folding kinetics indicating two-state folding behavior without detectable kinetic intermediates. A recent study, however, indicates a more complicated mechanism in which at least one intermediate becomes populated after the main rate-limiting step in folding (28). Consensus holds that partial α-helix structure is present in the transition state of GCN4 coiled-coil folding in which dimerization is promoted through interactions between monomers having preformed helices. These helices consist of a few turns in length and are encoded by the trigger sequence (15, 18, 25, 26, 29).

Crucial determinants of both monomer helix and coiled-coil formation are electrostatic interactions between charged residue side chains (30–35). The importance of such interactions in determining the specificity of GCN4 coiled-coil formation has been extensively studied and is well documented (reviewed in ref. 31). By contrast, the role of electrostatic interactions in general, and of salt bridges in particular, in coiled coil stability and folding remains a matter of debate. A number of experimental studies indicate favorable contributions to stability from electrostatic interactions (36), whereas others do not (37). We and others have suggested that an intramolecular Glu-22 to Arg-25 salt bridge within the trigger sequence plays a critical role in stabilizing the nascent α-helix structure at the C terminus that nucleates coiled-coil formation (18, 38). The remaining salt bridges appear to have roles in stabilizing the native state of the GCN4 leucine zipper rather than affecting the kinetics of coiled-coil folding (38). Here, we use a multidisciplinary approach including NMR, isothermal titration calorimetry (ITC), time-resolved CD spectroscopy, and mutagenesis to identify and characterize the features of the GCN4 trigger sequence that determine coiled-coil formation. Our findings provide a molecular basis for understanding coiled-coil formation in general.

Results

A Network of Interactions Stabilizes the Helical Structure of the GCN4 Coiled-Coil Trigger Sequence. To obtain insights into the interactions that initiate GCN4 leucine zipper formation we determined the NMR solution structure of a 16-residue peptide, denoted p16-31. This peptide contains the trigger sequence and thus serves as a tool to investigate the conformation of an early folding intermediate of coiled-coil formation (39). Helix formation by p16-31 is a monomolecular process and is not the result of dimerization, as judged from the lack of concentration dependence of CD and NMR spectra as well as analytical

Author contributions: M.O.S., I.J., A.T.A., and R.A.K. designed research; M.O.S., I.J., W.M.M., S.H., W.J., J.H.M., S.F., A.T.A., and R.A.K. performed research; M.O.S., I.J., A.T.A., and R.A.K. analyzed data; and M.O.S., I.J., A.T.A., and R.A.K. wrote the paper.

The authors declare no conflict of interest.

This article is a PNAS Direct Submission.

Abbreviations: HSQC, heteronuclear single quantum correlation; ITC, isothermal titration calorimetry.

Data deposition: The atomic coordinates have been deposited in the Protein Data Bank, www.pdb.org (PDB ID code 2OVN).

†To whom correspondence may be addressed. E-mail: michel.steinmetz@psi.ch or richard.kammerer@manchester.ac.uk.

This article contains supporting information online at www.pnas.org/cgi/content/full/0700321104/DC1.

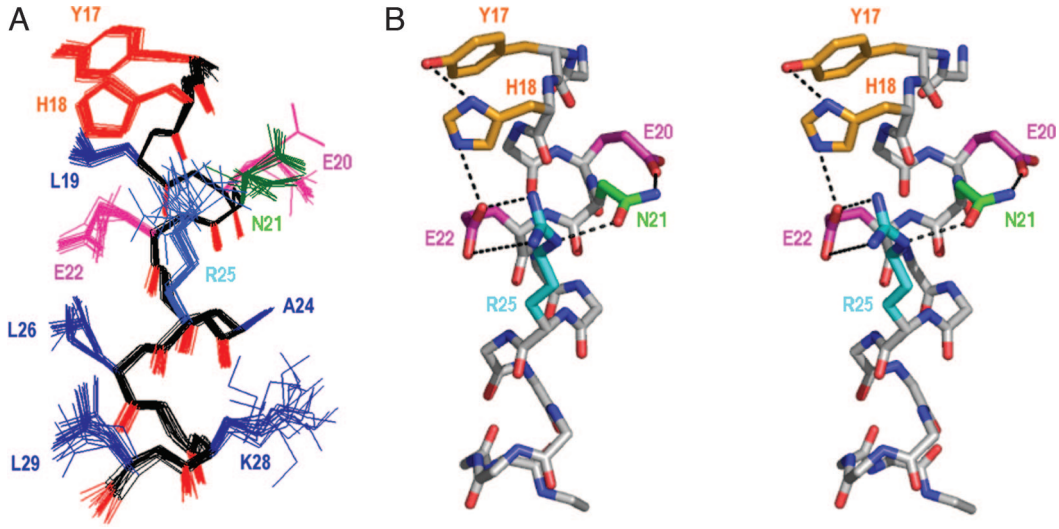

Fig. 1. The NMR solution structure of p16-31 reveals a network of side-chain interactions. (*A*) Best-fit superposition of the 20 lowest-energy NMR structures. The main chain is shown in black (carbons, nitrogens) and red (carbonyl oxygens). Selected side chains are shown in different colors and labeled according to their position in the GCN4 coiled-coil sequence (42). (*B*) Stereo side view of the p16-31 structure closest to the NMR ensemble average. Atoms of side chains forming the network of polar interactions are connected by dashed black lines.

ultracentrifugation at different peptide concentrations (15, 18, 40). NMR structures of the p16-31 peptide were calculated by using the restraints listed in supporting information (SI) Table 2. The trigger peptide adopts a regular α-helical conformation extending from residues His-18 to Lys-28 (Fig. 1*A* and SI Fig. 5). At the N terminus the α-helix is terminated by a nonclassical cap structure (41) involving a bifurcated hydrogen bond from the main-chain amide of Glu-20 to the carboxyl groups of Asn-16 and Tyr-17. A hydrogen bond between the aromatic groups of Tyr-17 and His-18 completes the cap (Fig. 1*B*). Notably, the main-chain structure of the trigger peptide between His-18 and Lys-28 is virtually identical to the corresponding regions of the two-stranded GCN4 coiled-coil crystal structure (42) with a backbone rmsd of only 0.6 ± 0.1 Å.

The most conspicuous feature seen in the NMR structure of the monomeric p16-31 trigger sequence peptide is a network of polar contacts involving residues Tyr-17, His-18, Glu-20, Asn-21, Glu-22, and Arg-25 (Fig. 1*B*). The critical role of Arg-25 in GCN4 leucine zipper formation (18, 38) can be explained by its central position within the network. The side chain of Arg-25 forms a hydrogen bond with Asn-21 and an ion pair with Glu-22, interactions that appear essential for establishing the network. The network is completed by side-chain contacts between His-18 and Glu-22, Glu-20 and Asn-21, and Tyr-17 and His-18. It should be noted that not all interactions are simultaneously seen in the 20 NMR structures of p16-31, suggesting a network involving several interchanging side-chain contacts (Fig. 1*A*). Consistent with this conclusion, a dynamic interplay of hydrogen-bonding and salt bridge interactions has also been observed in explicit solvent molecular dynamics simulations of p16-31 (40). Remarkably, several rearrangements of these interactions are seen in the dimeric GCN4 coiled-coil structure (Protein Data Bank ID code 2ZTA) and only those formed between Arg-25 and Glu-22, and between Glu-22 and His-18, are conserved. In addition to these intrahelical interactions, Glu-22 forms an interhelical salt bridge to Lys-27 of the neighboring GCN4 coiled-coil chain. The side chains of Tyr-17, Glu-20, and Asn-21 are not involved in interactions with other residues in the dimer.

To test the hypothesis that multiple charged groups contribute to the α-helix-stabilizing network of the trigger peptide, we further characterized the pH dependence of helical structure in p16-31 by following ^{1}Hα and ^{13}Cα chemical shifts in 10 ^{1}H-^{13}C heteronuclear single quantum correlation (HSQC) spectra collected between pH 1.5 and 12.5. The secondary ^{13}Cα chemical shifts of the peptide averaged over residues His-18 to Lys-28 indicate a progressive loss of α-helix structure from ≈60% at neutral pH to <10% with decreasing pH (Fig. 2*A*). This finding is quantitatively similar to the trend seen by CD spectroscopy (15, 18). The pH denaturation curve obtained from the averaged Cα chemical shifts of p16-31 is broad and appears slightly biphasic (Fig. 2*B*). The data can be fit to a single $pK_{a,app}$ of 5.6. The Hill coefficient, which gives a measure of the cooperativity of the apparent ionization equilibrium, has a value of $n = 0.38$, suggesting the involvement of multiple groups in the titration (43). Accordingly, the electrostatic interactions involving one or both of the negatively charged forms of Glu-20 and Glu-22 and the uncharged form of His-18 modulate the α-helical structure at neutral pH. An electrostatic interaction between Glu-22 and Arg-25 is also supported by the lesser pK_a of 4.14 ± 0.04 for Glu-22 compared with 4.30 ± 0.05 for Glu-20 (Fig. 2*C*), or random-coil-model compound values (ref. 44 and references therein). Further evidence for an interaction between Arg-25 and the glutamate residues is provided by the observation that the side-chain delta protons of Arg-25 sense the titration of the acidic residues (Fig. 2*D*) and that NOEs between the two residues appear at neutral, but not acidic, pH (SI Fig. 6).

On the whole, these data suggest that rather than a single interaction a interplay of multiple interactions contributes to helical stability of the monomeric early folding intermediate of GCN4 under conditions that otherwise promote leucine zipper folding.

Arg-25 Stabilizes Helical Structure of the Trigger Sequence and Accelerates GCN4 Coiled-Coil Folding. To analyze further the role of Arg-25 in the monomer helix formation of p16-31 and the folding and stability of the GCN4 leucine zipper, denoted GCN4-pWT, the following mutant peptides were prepared. (*i*) Arg-25 was mutated to alanine in a control trigger peptide and leucine zipper variant, denoted p16-31R25A and GCN4-pR25A, respectively, to exclude helix destabilization resulting from a lower helical propensity of the mutant residue compared with arginine. Alanine is reported to have the highest helix propensity in several monomeric peptides, at solvent-exposed positions in coiled coils and at exposed helical sites in proteins (reviewed

BIOPHYSICS

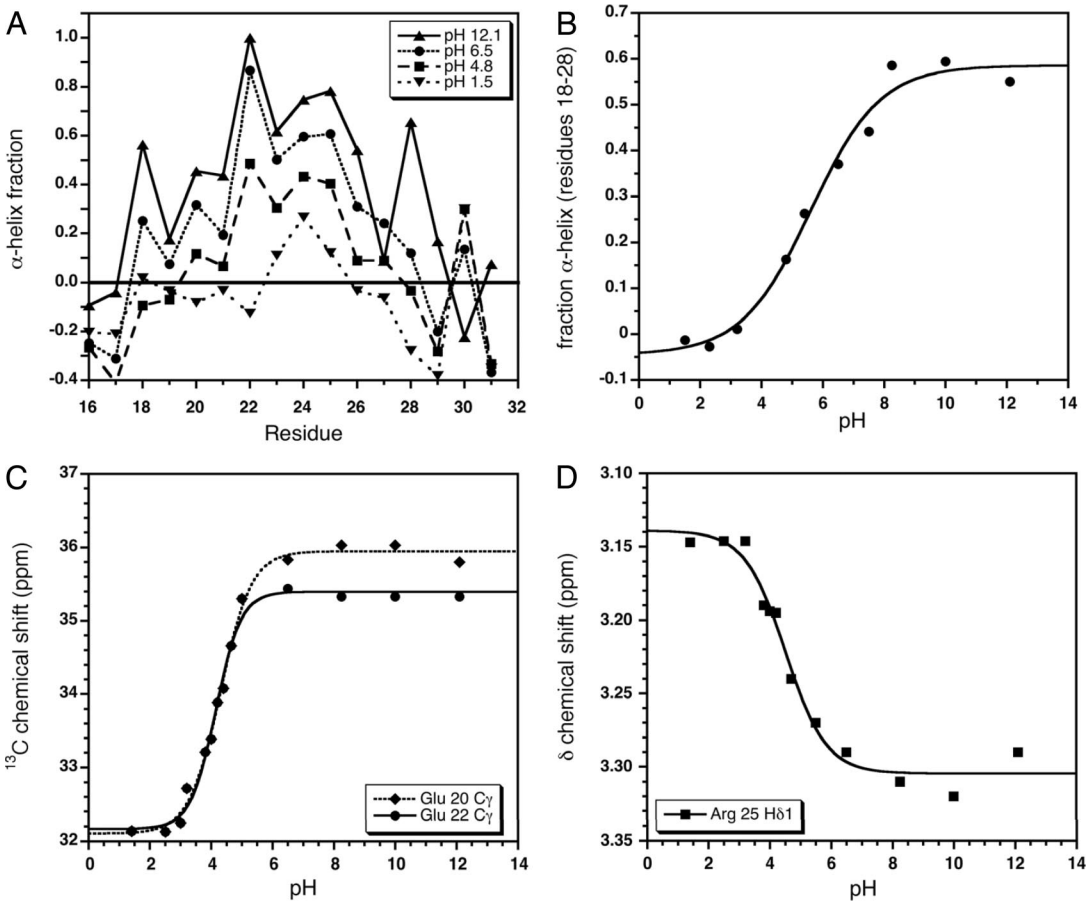

Fig. 2. Effects of pH on the stability of α-helix structure in the p16-31 peptide. (*A*) Sequence-specific profiles of α-helix content at four pH values. Estimates of fractional α-helix content were derived from ^{13}Cα chemical shifts in natural abundance ^{1}H-^{13}C HSQC spectra according to $[\delta_{observed} - \delta_{r.c.}]/[\delta_{GCN4\text{-}p1} - \delta_{r.c.}]$. (*B*) pH dependence of α-helix content from ^{13}Cα chemical shifts averaged over residues His-18 to Lys-28. The curve shows the fit of the data to a single apparent $pK_{a,app}$. (*C*) pH titration curves for the γ methylene carbons of Glu-20 and Glu-22. (*D*) Chemical shift changes of the downfield Arg-25 Hδ methylene protons as a function of pH. The protons sense the proximity of a titrating glutamate residue (Glu-22 based on the NMR structure; Fig. 1).

in ref. 31). (*ii*) Lysine mutant peptides, denoted p16-31R25K and GCN4-pR25K, were produced to probe the functional significance of the arginine guanidinium group with an alternative positively charged residue. (*iii*) To further assess the importance of α-helix propensity for coiled-coil formation, the threonine mutant GCN4-pR25T was prepared. Threonine has a low α-helical propensity because the residue's β-branched polar side chain is difficult to accommodate in a α-helix. (*iv*) To test whether the guanidinium group is important for stabilizing α-helix structure, Arg-25 was replaced by its isostere norleucine that mimics the hydrophobic moiety of the arginine side chain. None of the GCN4 leucine zipper mutants are expected to compromise coiled-coil formation because Arg-25 is located at a solvent-exposed exterior position remote from the dimer interface.

In initial experiments, the wild-type and mutant trigger sequence peptides were analyzed and compared by CD spectroscopy. As shown in Fig. 3*A*, the far-UV CD spectrum of the wild-type p16-31 peptide obtained at low temperature and physiological pH is characteristic of a polypeptide with ≈50% helical structure, consistent with the NMR analysis (Fig. 2*A*). The mutant peptides, p16-31R25A and p16-31R25K, show a shift of the minima from 205 to 201 nm in the CD spectrum (Fig. 3*A*), suggesting a substantial perturbation of the equilibrium from helix to random coil. This observation emphasizes the importance of the guanidium group for the stability of the monomeric α-helix at neutral pH. As shown in Fig. 3*B*, the helix content of wild-type and mutant peptides is also markedly decreased at acidic pH. Consistent with the NMR data (Fig. 2*A*), the titration profile of p16-31 measured from the change in ellipticity at 222 nm reveals a broad pH denaturation transition spanning ≈4 pH units that can be described by a single apparent $pK_{a,app}$ of 6.0 ± 0.2 (n = 0.33 ± 0.04; Fig. 3*B*). The pH titration data for p16-31R25K and p16-31R25A mutant peptides yielded apparent $pK_{a,app}$ values and Hill coefficients of 6.8 ± 0.1 (n = 0.39 ± 0.04) and 7.3 ± 0.1 (n = 0.46 ± 0.05), respectively, thus shifting the midpoints of acid-induced denaturation to higher pHs (Fig. 3*B*). A similar loss of α-helix structure at neutral pH was also observed in the ^{1}H-^{13}C HSQC NMR spectrum of p16-31R25A. The amount of residual helix content of the mutant is comparable to the one obtained for the wild-type peptide at acidic pH (SI Fig. 7). Together, these findings underscore the important role of Arg-25 in establishing the network of interactions required for GCN4 leucine zipper monomer helix stability.

To assess the significance of Arg-25 in the native coiled-coil dimer, the stabilities of the GCN4-pWT, GCN4-pR25A, GCN4-pR25T, GCN4-pR25Nle, and GCN4-pR25K leucine zipper variants were determined by following the change in ellipticity at 222 nm and 5°C as a function of total peptide concentration, by urea-induced unfolding or ITC dilution experiments (Table 1). Analyzing the data in terms of a two-state equilibrium between a dimer and monomer yielded the calculated free energies of unfolding, $\Delta G_{U,eq}$, listed in Table 1. The data indicate that the

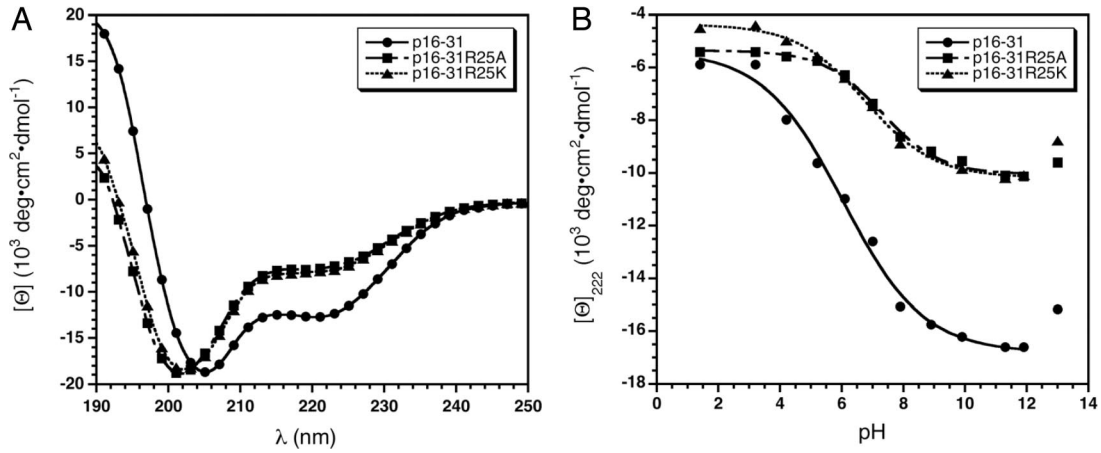

Fig. 3. Effects of Arg-25 substitutions on the stability of α-helix structure in the p16-31 peptide. (*A*) CD spectra of the wild-type p16-31 peptide compared with the p16-31R25K and p16-31R25A mutants. (*B*) pH dependence of mean residue ellipticity at 222 nm. The aberrant shifts in the titration curves above pH 12 are most likely caused by the beginning of the Arg-25 titration and were not included in the fits used to determine $pK_{a,app}$ values.

mutations destabilize the GCN4-pWT by 4–8 kJ·mol^{-1}, the arginine-to-threonine replacement being the most destabilizing as expected.

To dissect the contribution of Arg-25 to folding kinetics, the rate constants of refolding and urea unfolding were measured for wild-type and mutant GCN4 leucine zipper peptides by stop-flow CD at 222 nm (Fig. 4*A* and Table 1). For all of the variants $\Delta G_{U,kin}$ calculated from kinetic data and $\Delta G_{U,eq}$ obtained from equilibrium unfolding are in excellent agreement, supporting the validity of two-state folding. A comparison of the kinetic parameters listed in Table 1 reveals that the mutations decrease the refolding rate by factors ranging from 5 to 17. In contrast, the unfolding rates are conserved within a factor of 2 to 3. The mutations do not perturb the position of the folding transition state, as judged from the constancy of the Tanford's β_T value within the set. Rather the replacement of Arg-25 increases the activation energy barrier for folding. Surprisingly, the alanine and lysine mutations slow down folding to the same extent. This result, together with the structural data (Figs. 1–3), suggests that the characteristic features of the guanidinium group and not the positive charge *per se* is mainly responsible for stabilizing the network of interactions seen in the monomeric α-helix of the trigger sequence.

Discussion

Detailed knowledge of the folding mechanisms of coiled coils is crucial for exploiting their potential in a wide range of applications and understanding their functions in a large number of biological processes (1–13, 21–24). Here, we use the GCN4 leucine zipper as a model system to investigate fundamental principles underlying coiled-coil formation. The major aim of the present study was to identify and characterize in detail the molecular determinants that specify the α-helical conformation of the early monomeric GCN4 leucine zipper folding intermediate that drives coiled-coil formation. Previous work by us and others demonstrated that under physiological conditions partial α-helix formation in the trigger sequence monomer precedes coiled-coil assembly (14, 15, 18, 25, 26, 29). It is intuitive to assume that two such preformed and folding competent helices encompassing a few turns may form a nucleation site, which

Table 1. Kinetic and thermodynamic parameters of GCN4 leucine zipper peptides and Arg-25 mutants

Protein	$\Delta G_{U,eq}$	$k_f \times 10^{-4}$ [d]	k_u [e]	$\Delta G_{U,kin}$ [f]	$\Delta\Delta G_{\ddagger\to u}$ [g]	$\Delta\Delta G_{f\to\ddagger}$ [h]	$\Delta\Delta G_U$ [i]	$\lvert m_f\rvert$ [j]	$\lvert m_u\rvert$ [j]	β_T [k]
WT	33.3[a] 36.6[b]	66.3	0.17	35.0	0	0	0	0.76	0.44	0.63
R25A	27.8[a] 28.1[c]	12.0	0.44	29.0	3.91	2.14	6.05	0.93	0.38	0.71
R25T	25.5[a] 26.8[c]	3.8	0.52	25.8	6.63	2.52	9.15	0.79	0.44	0.64
R25Nle	n.d.	8.7	0.36	28.7	4.69	1.66	6.35	0.96	0.38	0.72
R25K	29.2[a]	12.5	0.34	29.6	3.42	1.36	4.78	0.81	0.41	0.66

Measurements were performed at 5°C (except ITC experiments, which were carried out at 20°C) in 10 mM sodium phosphate, pH 7.4, 150 mM NaCl. n.d., not determined.

[a]From the concentration dependence of $[\theta]_{222}$. Errors in ΔG_{eq} are ± 10%.

[b]From urea-induced unfolding.

[c]From dilution experiments by ITC.

[d]Units of $M^{-1}\cdot s^{-1}$. Errors are smaller than ± 10%.

[e]Units of s^{-1}. Errors are ± 10–20% depending on the length of extrapolation.

[f]Units of kJ·mol^{-1}. $\Delta G_{U,kin} = -RT\ln(k_u/k_f)$.

[g]Units of kJ·mol^{-1}. $\Delta\Delta G_{\ddagger\to u} = -RT\ln(k_f \text{ mutant}/k_f \text{ wild-type})$.

[h]$\Delta\Delta G_{f\to\ddagger} = -RT\ln(k_u \text{ wild-type}/k_u \text{ mutant})$.

[i]$\Delta\Delta G_U = \Delta\Delta G_{\ddagger\to u} + \Delta\Delta G_{f\to\ddagger}$.

[j]Units of M^{-1}. Errors are ± 0.05 M^{-1}.

[k]$\beta_T = 1 - m_{off}/(m_{on} + m_{off})$.

BIOPHYSICS

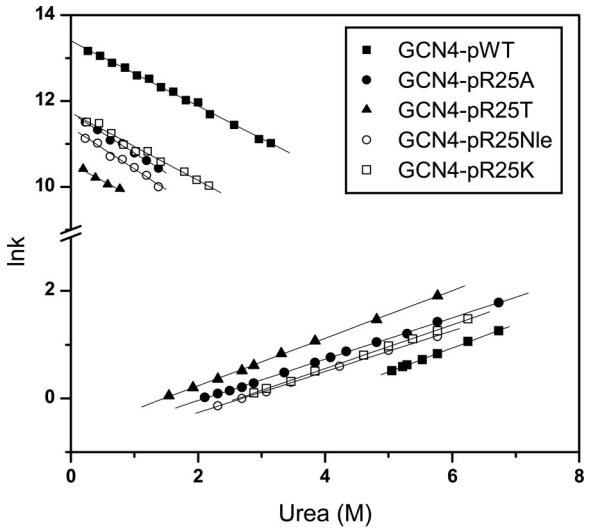

Fig. 4. Substitutions of Arg-25 significantly slows down folding of the GCN4 coiled coil. Microscopic rate constants were measured as a function of urea concentration. The fits to the data were calculated according to $\ln k_i^{urea} = \ln k_i^{water} + m_i[\text{urea}]$ (subscript i denotes folding or unfolding). Upper and lower symbols represent refolding and unfolding data, respectively. Parameters of the fits are listed in Table 1.

promotes productive in-register chain association. Interacting helices then "zip up" along the molecule to form the stable coiled-coil structure. Notably, this hierarchic folding mechanism (18, 45, 46) also provides a rational explanation for the efficient assembly of extensive coiled-coil domains (47) where chains are unlikely to align in-register if coiled-coil interactions form randomly along the sequence.

Our present findings reveal the important role of a dynamic network of interactions that includes Tyr-17, His-18, Glu-20, Asn-21, Glu-22, and Arg-25 in GCN4 coiled-coil folding by stabilizing the trigger sequence α-helix. This network is a characteristic feature of the monomeric GCN4 leucine zipper folding intermediate that is rearranged in the final dimeric coiled-coil structure. Notably, networks of intrahelical and interhelical electrostatic interactions are also the hallmark that distinguishes trigger sequences from other heptad repeat regions (17, 42). It is interesting to note that GCN4 coiled-coil folding markedly depends on solution conditions. The network of interactions in the GCN4 trigger sequence is pH sensitive, and helix structure is nearly abolished at acidic pH. This observation provides a possible explanation for the finding that the GCN4 coiled coil folds along multiple routes at pH 5.5 (25) where helix content within the trigger sequence is reduced significantly compared with neutral pH. Our present data together with the kinetic studies by Matthews and coworkers (26) indicate that GCN4 leucine zipper folds along a robust pathway at neutral pH when the helicity of the trigger sequence is maximal.

Although the trigger site concept for coiled-coil folding is generally accepted it has been noted that our previously proposed consensus sequence (15) is found only in a limited number of coiled-coil domains. The findings of the present study provide a rational explanation for the apparent discrepancy. It is well established that an α-helix can be stabilized through intramolecular interactions in many different ways and does not require a specific consensus sequence (32). The helical trigger sequences of different proteins show considerable diversity indicating that a consensus sequence is unlikely to exist. Supporting evidence for this conclusion is provided by Hodges and coworkers (48) who induced folding of a cortexillin/GCN4 hybrid lacking the canonical trigger sites by introducing stabilizing mutations that improved helicity without converting the sequence to the trigger consensus. Furthermore, we successfully demonstrated that a strategy employing networks of helix stabilizing interactions can be applied for the *de novo* design of uncommonly short and stable coiled coils (8, 49), emphasizing that the knowledge gained in this study has potential for applications using coiled-coil domains.

Materials and Methods

Peptide Preparation. GCN4 leucine zipper (Ac-Met-2-Glu-32-NH_2) and trigger (Ac-Asn-16-Gly-31-NH_2) peptides were prepared by using Fmoc solid-phase synthesis and purified by reversed-phase HPLC. Molecular masses were verified by mass spectrometry. Peptide concentrations were determined by tyrosine adsorption at 280 nm in 6 M GndHCl (50). All peptide concentrations are expressed as monomer equivalents.

NMR Spectroscopy. Samples for NMR work contained 3 mM p16-31 peptide and 10 mM sodium phosphate in 90% H_2O/10% D_2O. An Inova 600-MHz machine (Varian, Palo Alto, CA) fitted with a cryoprobe was used for all NMR experiments. Data were collected at 5°C. NMR resonances were assigned by the sequential walk method (51) using 2D NOESY (τ_m = 150 ms, 200 ms), total correlation spectroscopy (τ_m = 70 ms), primitive exclusive correlation spectroscopy, and natural abundance ^{1}H-^{13}C-HSQC and ^{1}H-^{15}N-HSQC spectra. Chemical shifts were referenced to internal 2,2-dimethyl-2-silapentane-5-sulfonate (52).

Restraints for structure calculations were collected on a peptide sample at pH 7.5. Distance restraints were grouped into three ranges (1.8–2.7, 1.8–3.5, and 1.8–5.0 Å) based on the intensities of NOE cross-peaks. Standard α-helix hydrogen bonds ON(i, i + 4) and ϕ dihedral angle restraints ($-60 \pm 30°$) were included for residues 17–24 based on lowered $^3J_{HNH\alpha}$ coupling constants in primitive exclusive correlation spectroscopy experiments, secondary Cα, Hα chemical shifts, and patterns of short-range NOEs consistent with α-helix structure (SI Fig. 5). NMR structure calculations started from 200 models with randomized dihedral angles. Structures were calculated with the program X-PLOR (version 3.851) according to a published protocol (53). The 20 lowest energy structures were kept for analyses. The final structures had no distance violations >0.3 Å or dihedral violations >3°.

Natural abundance sensitivity-enhanced 2D ^{13}C-HSQC and 1D ^{13}C-edited experiments were used to obtain pH titration data. Random coil reference values for calculations of helix content were taken from the literature (54). The parameters pK_a (ionization constant), δ_{low} (low pH chemical shift plateau), δ_{high} (high pH chemical shift plateau), and n (Hill coefficient) were determined from nonlinear least-squares fits of the chemical shift (δ) data as a function of pH to a modified Henderson–Hasselbach equation (55).

Other Biophysical Methods. CD experiments were performed on a J-715 instrument (Jasco, Easton, MD). Conformational transitions were followed at 222 nm and 5°C. The concentration dependence of the CD signal was measured for 1–500 μM peptide, and the data were processed to obtain K_U and ΔG_U as described (56). Urea denaturation curves were measured with 25 μM peptide. Data were analyzed by nonlinear regression according to well established procedures (57).

ITC dilution experiments were performed at 20° with a VP-ITC microcalorimeter (MicroCal, Amherst, MA). Peptide

concentration in the injection syringe was 500–600 μM. Injection volume was 10 or 20 μl. The resulting dilution isotherm was processed as described (58).

Kinetic experiments were performed with the π^*-180 instrument (Applied Photophysics, Surrey, U.K.) at 5°C. Mixing ratios of protein/buffer of 1:10 or 1:25 were used. Final protein concentration was 15–35 μM. At least 10 firings were averaged for each kinetic trace. The rates of folding and unfolding were calculated by numerical integration of the differential equations describing the time course of dimer and monomer concentration change, as implemented in the program DynaFit.

All experiments were performed in 10 mM sodium phosphate, 150 mM NaCl, pH 7.4. Urea concentrations were verified by measuring the refractive index.

We thank Dr. C. Garcia-Echeverría (Novartis Pharma) for supplying the wild-type and mutant p16-31 peptides. M.O.S. and I.J. were supported by Swiss National Science Foundation Grant 3100A0-109423 (to M.O.S.) and within the framework of the National Center of Competence in Research Structural Biology program (I.J.). A.T.A. was supported by National Science Foundation Grant MB 0236316 and the National Institutes of Health–National Center for Research Resources. W.M.M. was supported by a summer research stipend from the Richard C. Crain, Jr. Memorial Fellowship Fund. R.A.K. is a Wellcome Trust Senior Research Fellow in Basic Biomedical Science.

1. Kohn WD, Hodges RS (1998) *Trends Biotechnol* 16:379–389.
2. Eckert DM, Kim PS (2001) *Proc Natl Acad Sci USA* 98:11187–11192.
3. Cho CH, Kammerer RA, Lee HJ, Steinmetz MO, Ryu YS, Lee SH, Yasunaga K, Kim KT, Kim I, Choi HH, *et al.* (2004) *Proc Natl Acad Sci USA* 101:5547–5552.
4. Petka WA, Harden JL, McGrath KP, Wirtz D, Tirrell DA (1998) *Science* 281:389–392.
5. Ryadnov MG, Ceyhan B, Niemeyer CM, Woolfson DN (2003) *J Am Chem Soc* 125:9388–9394.
6. Rieker JD, Hu JC (2000) *Methods Enzymol* 328:282–296.
7. Arndt KM, Muller KM, Pluckthun A (2001) *J Mol Biol* 312:221–228.
8. Kammerer RA, Kostrewa D, Zurdo J, Detken A, Garcia-Echeverria C, Green JD, Muller SA, Meier BH, Winkler FK, Dobson CM, *et al.* (2004) *Proc Natl Acad Sci USA* 101:4435–4440.
9. Severin K, Lee DH, Kennan AJ, Ghadiri MR (1997) *Nature* 389:706–709.
10. Contegno F, Cioce M, Pelicci PG, Minucci S (2002) *Proc Natl Acad Sci USA* 99:1865–1869.
11. Wang C, Stewart RJ, Kopecek J (1999) *Nature* 397:417–420.
12. Ruch C, Skiniotis G, Steinmetz MO, Walz T, Ballmer-Hofer K (2007) *Nat Struct Mol Biol* 14:249–250.
13. Raman S, Machaidze G, Lustig A, Aebi U, Burkhard P (2006) *Nanomedicine* 2:95–102.
14. Steinmetz MO, Stock A, Schulthess T, Landwehr R, Lustig A, Faix J, Gerisch G, Aebi U, Kammerer RA (1998) *EMBO J* 17:1883–1891.
15. Kammerer RA, Schulthess T, Landwehr R, Lustig A, Engel J, Aebi U, Steinmetz MO (1998) *Proc Natl Acad Sci USA* 95:13419–13424.
16. Frank S, Lustig A, Schulthess T, Engel J, Kammerer RA (2000) *J Biol Chem* 275:11672–11677.
17. Burkhard P, Kammerer RA, Steinmetz MO, Bourenkov GP, Aebi U (2000) *Struct Fold Des* 8:223–230.
18. Kammerer RA, Jaravine VA, Frank S, Schulthess T, Landwehr R, Lustig A, Garcia-Echeverria C, Alexandrescu AT, Engel J, Steinmetz MO (2001) *J Biol Chem* 276:13685–13688.
19. Bosshard HR, Durr E, Hitz T, Jelesarov I (2001) *Biochemistry* 40:3544–3552.
20. Meisner WK, Sosnick TR (2004) *Proc Natl Acad Sci USA* 101:13478–13482.
21. Lupas AN, Gruber M (2005) *Adv Protein Chem* 70:37–38.
22. Parry DA (2005) *Adv Protein Chem* 70:113–142.
23. Burkhard P, Stetefeld J, Strelkov SV (2001) *Trends Cell Biol* 11:82–88.
24. Mason JM, Arndt KM (2004) *Chembiochem* 5:170–176.
25. Moran LB, Schneider JP, Kentsis A, Reddy GA, Sosnick TR (1999) *Proc Natl Acad Sci USA* 96:10699–10704.
26. Zitzewitz JA, Ibarra-Molero B, Fishel DR, Terry KL, Matthews CR (2000) *J Mol Biol* 296:1105–1116.
27. Holtzer ME, Bretthorst GL, d'Avignon DA, Angeletti RH, Mints L, Holtzer A (2001) *Biophys J* 80:939–951.
28. Wang T, Lau WL, DeGrado WF, Gai F (2005) *Biophys J* 89:4180–4187.
29. Myers JK, Oas TG (1999) *J Mol Biol* 289:205–209.
30. Bosshard HR, Marti DN, Jelesarov I (2004) *J Mol Recognit* 17:1–16.
31. Woolfson DN (2005) *Adv Protein Chem* 70:79–112.
32. Munoz V, Serrano L (1995) *Curr Opin Biotechnol* 6:382–386.
33. Hodges RS (1996) *Biochem Cell Biol* 74:133–154.
34. Chakrabartty A, Baldwin RL (1995) *Adv Protein Chem* 46:141–176.
35. Kammerer RA, Kostrewa D, Progias P, Honnappa S, Avila D, Lustig A, Winkler FK, Pieters J, Steinmetz MO (2005) *Proc Natl Acad Sci USA* 102:13891–13896.
36. Lavigne P, Sonnichsen FD, Kay CM, Hodges RS (1996) *Science* 271:1136–1138.
37. Lumb KJ, Kim PS (1995) *Science* 268:436–439.
38. Ibarra-Molero B, Zitzewitz JA, Matthews CR (2004) *J Mol Biol* 336:989–996.
39. Religa TL, Markson JS, Mayor U, Freund SM, Fersht AR (2005) *Nature* 437:1053–1056.
40. Missimer JH, Steinmetz MO, Jahnke W, Winkler FK, van Gunsteren WF, Daura X (2005) *Chem Biodivers* 2:1086–1104.
41. Aurora R, Rose GD (1998) *Protein Sci* 7:21–38.
42. O'Shea EK, Klemm JD, Kim PS, Alber T (1991) *Science* 254:539–544.
43. Markley JL (1975) *Acc Chem Res* 8:70–80.
44. Thurlkill RL, Grimsley GR, Scholtz JM, Pace CN (2006) *Protein Sci* 15:1214–1218.
45. Baldwin RL, Rose GD (1999) *Trends Biochem Sci* 24:77–83.
46. Baldwin RL, Rose GD (1999) *Trends Biochem Sci* 24:26–33.
47. Mo JM, Holtzer ME, Holtzer A (1991) *Proc Natl Acad Sci USA* 88:916–920.
48. Lee DL, Lavigne P, Hodges RS (2001) *J Mol Biol* 306:539–553.
49. Kammerer RA, Steinmetz MO (2006) *J Struct Biol* 155:146–152.
50. Edelhoch H (1967) *Biochemistry* 6:1948–1954.
51. Wuthrich K (2003) *Angew Chem Int Ed Engl* 42:3340–3363.
52. Wishart DS, Bigam CG, Yao J, Abildgaard F, Dyson HJ, Oldfield E, Markley JL, Sykes BD (1995) *J Biomol NMR* 6:135–140.
53. Gronenborn AM, Filpula DR, Essig NZ, Achari A, Whitlow M, Wingfield PT, Clore GM (1991) *Science* 253:657–661.
54. Wishart DS, Bigam CG, Holm A, Hodges RS, Sykes BD (1995) *J Biomol NMR* 5:67–81.
55. Dames SA, Kammerer RA, Moskau D, Engel J, Alexandrescu AT (1999) *FEBS Lett* 446:75–80.
56. Betz S, Fairman R, O'Neil K, Lear J, Degrado W (1995) *Philos Trans R Soc London B* 348:81–88.
57. Santoro MM, Bolen DW (1988) *Biochemistry* 27:8063–8068.
58. Burrows SD, Doyle ML, Murphy KP, Franklin SG, White JR, Brooks I, McNulty DE, Scott MO, Knutson JR, Porter D, *et al.* (1994) *Biochemistry* 33:12741–12745.